TOXICOLOGICAL SCIENCES **136(2)**, 467–477 2013
doi:10.1093/toxsci/kft214
Advance Access publication September 30, 2013

Uptake, p53 Pathway Activation, and Cytotoxic Responses for Co(II) and Ni(II) in Human Lung Cells: Implications for Carcinogenicity

Samantha E. Green, Michal W. Luczak,[1] Jessica L. Morse, Zachary DeLoughery, and Anatoly Zhitkovich[2]

Department of Pathology and Laboratory Medicine, Brown University, Providence, Rhode Island 02912

[1]M. W. Luczak is on leave from the Department of Pediatric Gastroenterology and Metabolic Diseases, Poznan University of Medical Sciences, Poznan, Poland.

[2]To whom correspondence should be addressed at Department of Pathology and Laboratory Medicine, Brown University, 70 Ship Street, Room 507, Providence, RI 02912. Fax: (401) 863-9008. E-mail: anatoly_zhitkovich@brown.edu.

Received July 22, 2013; accepted September 6, 2013

Cobalt(II) and nickel(II) ions display similar chemical properties and act as hypoxia mimics in cells. However, only soluble Co(II) but not soluble Ni(II) is carcinogenic by inhalation. To explore potential reasons for these differences, we examined responses of human lung cells to both metals. We found that Co(II) showed almost 8 times higher accumulation than Ni(II) in H460 cells but caused a less efficient activation of the transcriptional factor p53 as measured by its accumulation, Ser15 phosphorylation, and target gene expression. Unlike Ni(II), Co(II) was ineffective in downregulating the p53 inhibitor MDM4 (HDMX). Co(II)-treated cells continued DNA replication at internal doses that caused massive apoptosis by Ni(II). Apoptosis and the overall cell death by Co(II) were delayed and weaker than by Ni(II). Inhibition of caspases but not programmed necrosis pathways suppressed Co(II)-induced cell death. Knockdown of p53 produced 50%–60% decreases in activation of caspases 3/7 and expression of 2 most highly upregulated proapoptotic genes PUMA and NOXA by Co(II). Overall, p53-mediated apoptosis accounted for 55% cell death by Co(II), p53-independent apoptosis for 20%, and p53/caspase-independent mechanisms for 25%. Similar to H460, normal human lung fibroblasts and primary human bronchial epithelial cells had several times higher accumulation of Co(II) than Ni(II) and showed a delayed and weaker caspase activation by Co(II). Thus, carcinogenicity of soluble Co(II) could be related to high survival of metal-loaded cells, which permits accumulation of genetic and epigenetic abnormalities. High cytotoxicity of soluble Ni(II) causes early elimination of damaged cells and is expected to be cancer suppressive.

Key Words: **cobalt; nickel; toxicity; cancer; TP53; apoptosis.**

Cobalt (Co) is a toxic metal with significant public health concerns associated with its occupational exposures and release by commonly used cobalt-chromium hip prostheses (Delaunay *et al.*, 2010; Nordberg, 1994; Simonsen *et al.*, 2012). Metallic and other forms of Co are used in numerous industrial applications such as electroplating, in manufacturing of high-temperature alloys, diamond polishing tools, carbides, and hard metals, and as catalysts and pigments. Exposure to Co can result in a series of adverse health effects that include impaired thyroid function, cardiomyopathy, polycythemia, and neurotoxicity. In the inhalation exposures, the main target of Co toxicity is the respiratory system. Occupationally exposed workers are at risk of developing interstitial lung fibrosis, alvelolytis, and asthma. These and other toxic effects have also been found in the respiratory tract of rodents after chronic inhalation of Co(II) (Bucher *et al.*, 1990). The 2-year inhalation study by the National Toxicology Program (NTP) found strong evidence for carcinogenicity of soluble Co(II) (cobalt sulfate) in the lungs of mice and rats (Bucher *et al.*, 1999). Occupational exposures to certain Co-containing materials have also been associated with elevated risks of lung cancers (Simonsen *et al.*, 2012). The mechanisms of lung carcinogenicity by Co(II) are currently poorly understood. Co(II) is clastogenic in mammalian cells but only weakly mutagenic in the Ames reversion assay (De Boeck *et al.*, 2003).

Ni(II)-containing compounds are classified as carcinogenic to humans (Goodman *et al.*, 2011; Muñoz and Costa, 2012; Salnikow and Zhitkovich, 2008). Inhalation exposures to particulate Ni(II) forms have been found to cause respiratory tumors in humans and rodents. Although the intracellular release of Ni(II) ions is generally believed to be responsible for carcinogenic activity of the particulate forms, soluble Ni(II) (nickel sulfate) was inactive in the 2-year inhalation study by the NTP (Dunnick *et al.*, 1995) and epidemiological findings for soluble Ni(II) have largely been negative (Goodman *et al.*, 2011). Ni(II) and Co(II) are adjacent members of the first series of transition metals and they have similar ionic radii and other chemical properties. Both metals act as chemical hypoxia mimics by activating the hypoxia-responsive transcriptional factor HIF-1 (Salnikow *et al.*, 2000, 2004; Wang and Semenza, 1995) and can catalyze Fenton-type reactions with hydrogen peroxide when complexed with appropriate ligands (Huang *et al.*, 1995;

Van den Broeke *et al.*, 1998). Ni(II) and Co(II) display strong binding affinity for soft-type ligands such as sulfur and nitrogen (Nieboer and Richardson, 1980). This ligand preference is responsible for the ability of Co(II) and Ni(II) to displace Zn(II) from zinc-finger proteins such as the DNA repair factor XPA (Bal *et al.*, 2003; Kopera *et al.*, 2004). Thus, based on many chemical and biological similarities, one could expect that soluble Co(II) and Ni(II) forms should have similar carcinogenic properties, which was clearly not the case in the NTP inhalation studies (Bucher *et al.*, 1999; Dunnick *et al.*, 1995).

In order to understand potential reasons for different respiratory carcinogenicity of soluble Co(II) and Ni(II), we conducted a detailed study of uptake, stress responses, and survival of human lung cells treated with these metals. We found that human lung cells displayed several times higher accumulation of Co(II) but showed a delayed and weaker activation of replication checkpoint, the stress-responsive transcription factor p53, and apoptosis. In contrast, Ni(II) induced a rapid and more robust apoptosis associated with a much earlier activation of p53. High tolerance of Co(II) by human lung cells, permitting DNA replication and survival despite massive internal doses of this redox-active metal, can promote accumulation of genetic damage and helps explain its lung carcinogenicity.

MATERIALS AND METHODS

Chemicals. $CoCl_2{\cdot}6H_2O$ (BioReagent grade), $NiCl_2{\cdot}6H_2O$ (BioReagent grade), and nitric acid (>99.999% purity) were obtained from Sigma-Aldrich. QVD-Oph was purchased from Imgenex. E64d, cyclosporin A, necrostatin-1, and ALLN were from Santa Cruz Biotechnology. All other reagents were purchased from Sigma-Aldrich.

Cells and treatments. H460 human lung epithelial cells were purchased from the American Type Culture Collection (ATCC) and maintained in RPMI-1640 medium (Gibco 11875-093) supplemented with 10% fetal bovine serum and penicillin/streptomycin. IMR90 human lung fibroblasts were obtained from ATCC and propagated in Dulbecco's modified Eagle medium (Gibco 12430-062) containing 15% serum and antibiotics. Primary human bronchial epithelial (HBE) cells were obtained from Lonza and maintained in serum-free basal medium (Lonza CC-3170) supplemented with growth factors and standard antibiotics. H460 and HBE cells were grown in 95% air/5% CO_2, whereas IMR90 fibroblasts were kept in 5% O_2 and 5% CO_2. Exposure to metals was usually done in the complete growth media except for experiments with measurements of extracellular LDH immediately after 24-h exposures when serum-free media were used. Stock solutions of $CoCl_2$ and $NiCl_2$ were freshly prepared in deionized water and filter sterilized before addition to cells.

Small hairpin RNA. The pSUPER-RETRO vector was used for a stable downregulation of p53 expression in H460 cells. Empty and scrambled small hairpin RNA (shRNA)–coding vectors were obtained from Oligoengine. The p53-targeting sequence was GACTCCAGTGGTAATCTAC. Retrovirus packaging, infections, and puromycin selection have been described previously (Reynolds *et al.*, 2004). Cells infected with control and targeting vectors were grown in a media containing 1.5 μg/ml puromycin.

Western blotting. Soluble cellular proteins were extracted as described previously (Reynolds and Zhitkovich, 2007). Proteins were separated by SDS-poly-acrylamide gel electrophoresis and electrotransferred to ImmunoBlot PVDF membrane (Bio-Rad). Primary antibodies for PARP (9542), pS15-p53 (9284), pS46-p53 (2521), cleaved caspase-3 (9661), cleaved caspase-7 (8438), BCL2 (2870), BCL-X_L (2764), MCL1 (5453), and pS70-BCL2 (2827) were from Cell Signaling Technology; for p21 (SX118) from BD Biosciences; for MDM4 (A300-287A) from Bethyl Laboratories; for p53 (DO-1) from Santa Cruz Biotechnology; and for γ-tubulin (T6557) from Sigma.

Cytotoxicity. Cell death was assessed by measurements of leakage of cellular lactate dehydrogenase (LDH) into media. LDH activity was determined by a commercial kit (Cayman Chemical). Cells were seeded into 96-well plates (10 000–20 000 cells/well) and treated with metals the next day. Due to high LDH levels in serum, cells were incubated in serum-free media for the determination of leaked cellular LDH. At the collection times, plates were centrifuged at 400 × g for 5 min, and media were aspirated for the determination of leaked LDH according to the manufacturer's instructions. With the exception of the initial experiments in Figure 2, the amount of LDH leaked into the media was expressed as a percentage of total (leaked and cellular) LDH activity in each sample. Cellular LDH activity was determined after removal of growth medium and lysis of cells in fresh RPMI-1640 medium containing 0.1% Triton X-100 (10 min, room temperature). Cytotoxic effects of metals were also examined by the determinations of metabolic activity of cell populations using the CellTiter-Glo luminescent cell viability assay (Promega), which quantifies cellular ATP levels. These measurements integrate the size of cell populations and metabolic activity of individual cells, making it sensitive to all forms of cytotoxicity, such as growth arrest, cell death of any kind, and impairment of cellular metabolic activity. H460 cells were seeded into black 96-well optical bottom cell culture plates (2000 cells/well) and grown overnight prior to the addition of metals. The assay reagents were added to the plates, and luminescence measurements were recorded after 10-min incubation at room temperature. Caspase 3/7 activity was measured by a luminescence-based kit from Promega. Cells were seeded into 96-well plates (2000 cells/well) and treated with metals the next day. Caspase activity assay was performed as recommended by the manufacturer.

Clonogenic survival. A long-term survival of metal-treated cells was assessed by clonogenic assay, which measures the ability of individual cells to retain long-term proliferative activity and produce colonies. For determination of a role of p53 in clonogenic viability, sh-SCR and sh-p53 H460 cells were seeded onto 60-mm dishes (400 cells/dish) and treated with metals for 24 h on the next day. At 7–8 days postexposure, cells were fixed with methanol and stained with a commercial Giemsa solution (Sigma-Aldrich). Colonies containing 30 or more cells were scored. In clonogenic experiments comparing Co(II) and Ni(II) toxicity, H460 cells were treated with metals for 24 h in mass cultures as described in uptake studies. Floating and attached cells were combined and 400 cells/dish were seeded for the determination of clonogenic survival.

Quantitation of attached cells. The number of attached cells was determined using the CyQUANT reagent from Invitrogen. At the indicated times, media were removed and cells were incubated with a DNA-staining solution for 30 min at 37°C. Fluorescence readings were recorded with 485 nm excitation and 530 nm emission settings.

Quantitative reverse transcriptase PCR. Total RNA from H460 cells was isolated using a TRIzol reagent (Invitrogen). Purity of RNA samples was assessed by a Nanodrop spectrophotometer. Complementary DNA was synthesized by the RT First Strand kit as instructed by the manufacturer (SABiosciences). PCR reactions were performed using primers from SABiosciences and the ABI 7900HT Real-Time PCR system (Applied Biosystems). The housekeeping genes B2M, HPRT1, RPLPO, and ACTB were used for normalization purposes. Differences in gene expression were calculated by the $2^{-\Delta\Delta Ct}$ method.

Cellular uptake of metals. Cellular amounts of Co and Ni were determined by graphite furnace atomic absorption spectroscopy (GF-AAS) using nitric acid extracts. Cells were seeded into 6-well plates (H460: 3×10^5 cells/well; IMR90 and HBE: 2×10^5 cells/well) and treated with metals the next day. After removal of metal-containing media, attached cells were washed twice with warm PBS and collected by trypsinization in the presence of EDTA (Gibco 15400-054 Trypsin-EDTA solution). After 2 washes with ice-cold PBS, cells were resuspended in 50 μl of deionized water followed by mixing with the equal volume of 10% nitric acid. Samples were then frozen at −80°C,

thawed at 37°C, heated for 60 min at 50°C, and placed on ice for 30 min. Metal-containing supernatants were collected after centrifugation at 10 000 × g for 10 min at 4°C. The extracts were diluted to 2% nitric acid for metal analysis by GF-AAS (AAnalyst600 Atomic Absorption Spectrometer, Perkin-Elmer). Cellular precipitates formed after metal extraction were washed twice with ice-cold 5% nitric acid, centrifuged at 10 000 × g for 5 min at 4°C, and dissolved in 100 µl of 0.5M NaOH at 37°C for 30 min. The protein amount in the solubilized cellular material was used for normalization of metal uptake. In analytical recovery experiments, 0.5 and 2.5 nmol Co and Ni were added to 0.5 million H460 cells suspended in 50 µl water immediately followed by the standard procedure for metal extraction by nitric acid. Control samples containing no cells were processed in parallel. To assess the effectiveness of the nitric acid extraction of metals in uptake experiments, H460 cells were treated with 200µM Co(II) and 400µM Ni(II) for 6 h, processed by the standard protocol, and then metals were measured in both nitric acid extracts and nitric acid–insoluble material solubilized in 0.5mM NAOH. The effectiveness of extraction was expressed as a percentage of total cellular metals that were present in the nitric acid–soluble fractions.

Fluorescence-activated cell sorting. After removal of metal-containing media, cells were labeled with 10µM 5-ethynyl-2′-deoxyuridine (EdU) for 30 min. Cells were washed with PBS, collected by trypsinization, and fixed overnight in 80% ethanol at 4°C. PBS-washed cells were permeabilized with 0.5% Triton X-100 in PBS for 30 min at room temperature. After a wash with 2 ml PBS, cells were resuspended in 150 µl EdU Click-iT reaction cocktail from Invitrogen (Click-iT EdU-Alexa Fluor 488 Flow Cytometry Assay) and incubated for 30 min at room temperature in the dark. Cells were washed once with 2 ml PBS, resuspended in 500 µl PBS containing 4 µg/ml propidium iodide, and incubated for 30 min at room temperature protected from light. Cells were washed once with 2 ml PBS and resuspended in 0.5 ml PBS for flow cytometry analysis (FACSCalibur, BD Biosciences). Data were analyzed by CellQuest Pro software.

Statistics. *p* values were calculated using 2-tailed, unpaired *t* test.

RESULTS

Metal Uptake and p53 Activation by Co(II) and Ni(II) in H460 Cells

Lung is the main target of toxic effects by Co(II) and Ni(II) in occupational settings (Goodman *et al.*, 2011; Nordberg, 1994). The NTP inhalation studies found that soluble Co(II) and insoluble Ni(II) produced lung tumors originated from epithelial cells (Bucher *et al.*, 1999; Dunnick *et al.*, 1995). Therefore, we chose H460 human lung cells as our primary cell model. These cells retained epithelial morphology and showed a normal activation of the stress-responsive transcription factor p53 by Ni(II) (Wong *et al.*, 2013) and other lung toxicants and carcinogens (Reynolds and Zhitkovich, 2007; Wong *et al.*, 2012; Zhang *et al.*, 2006). Co and Ni are high-dose carcinogens producing respiratory tumors at doses that cause death of significant amounts of lung cells (Bucher *et al.*, 1999; Dunnick *et al.*, 1995; Goodman *et al.*, 2011). It has been calculated that millimolar intracellular concentrations of these metals are necessary for cell transformation (Goodman *et al.*, 2011; Muñoz and Costa, 2012). In our experiments, we tested a range of Ni and Co concentrations that included weakly (< 25% decrease in long-term cell viability) and strongly (> 50% decrease in long-term viability) cytotoxic doses. Strongly cytotoxic doses provide sufficiently robust responses that are necessary for reliable assessments of partial effects of genetic or pharmacological manipulations.

To accurately assess a relative toxicity of Ni(II) and Co(II), it was important to determine cellular accumulation of both metals under our exposure conditions. We adapted a nitric acid–based extraction procedure that was developed for measurements of cellular chromium (Messer *et al.*, 2006). GF-AAS analyses of extracts from "spiked" H460 cells found higher than 90% analytical recovery for both metals (Fig. 1A). The effectiveness of the nitric acid protocol in extraction of both Co and Ni from metal-exposed H460 cells exceeded 95% (Fig. 1B). Uptake measurements in H460 cells treated with metals for 6 h showed a much higher accumulation of Co in comparison to Ni (Fig. 1C). On average, cells accumulated 7.7 times more Co. To compare the abilities of Co(II) and Ni(II) in activation of the transcriptional factor p53, we examined its protein and Ser15 phosphorylation levels. Activation of several stress-responsive kinases can lead to phosphorylation of Ser15, which usually correlates with increased protein stability of p53 (Kruse and Gu, 2009; Toledo and Wahl, 2006). We found that Co(II) caused only marginal increases in p53 protein and its Ser15 phosphorylation at the highest dose, whereas Ni(II) produced a very clear upregulation of both p53 readouts (Fig. 1D). At maximal doses that were tested, p53 levels were increased 4.4-fold by Ni, but only 1.4-fold by Co(II), despite its 4.4 times higher cellular accumulation. Next, we investigated how H460 cells respond to metals after 24-h-long exposures. A much greater uptake of Co, averaging 8.6-fold from the slopes of dose-response curves, was detected again (Fig. 1E). Compared with 6-h treatments, cellular levels of Ni and Co were, respectively, 1.6 and 1.8 times higher, demonstrating a significant additional influx of both metals. Activation of p53 by Co(II) after 24-h exposures was clearly evident, with particularly strong increases in its protein and Ser15 phosphorylation levels at 400µM dose (Fig. 1F). Induction of the p53 target, the CDK inhibitor p21 (CDKN1A), showed similar Co(II) dose responses by Western blots and quantitative reverse transcriptase PCR (qRT-PCR; Figs. 1F and 1G). A complete loss of p21 messenger RNA (mRNA) upregulation by Co(II) in cells with a stable p53 knockdown by shRNA confirmed the p53 dependence of p21 induction (Fig. 1G). Expression of another target gene MDM2 was induced by Co(II) in control but not in p53-depleted cells, provided further evidence for p53 activation (Fig. 1G). When compared on the basis of their intracellular doses, Co(II) was still a weaker activator of the p53 pathway than Ni(II). For example, despite their 3.3 times higher metal accumulation, 200µM Co(II)-treated cells had lower p53 and p21 levels than 300µM Ni(II) samples (Fig. 1F). Striking differences between 2 metals were also found in modulation of the p53 transactivation inhibitor MDM4 (HDMX). Ni(II)-exposed cells showed severely depressed levels of MDM4 protein with less than 10% remaining amount for the 300µM treatment, whereas even the highest concentration of 400µM Co(II)

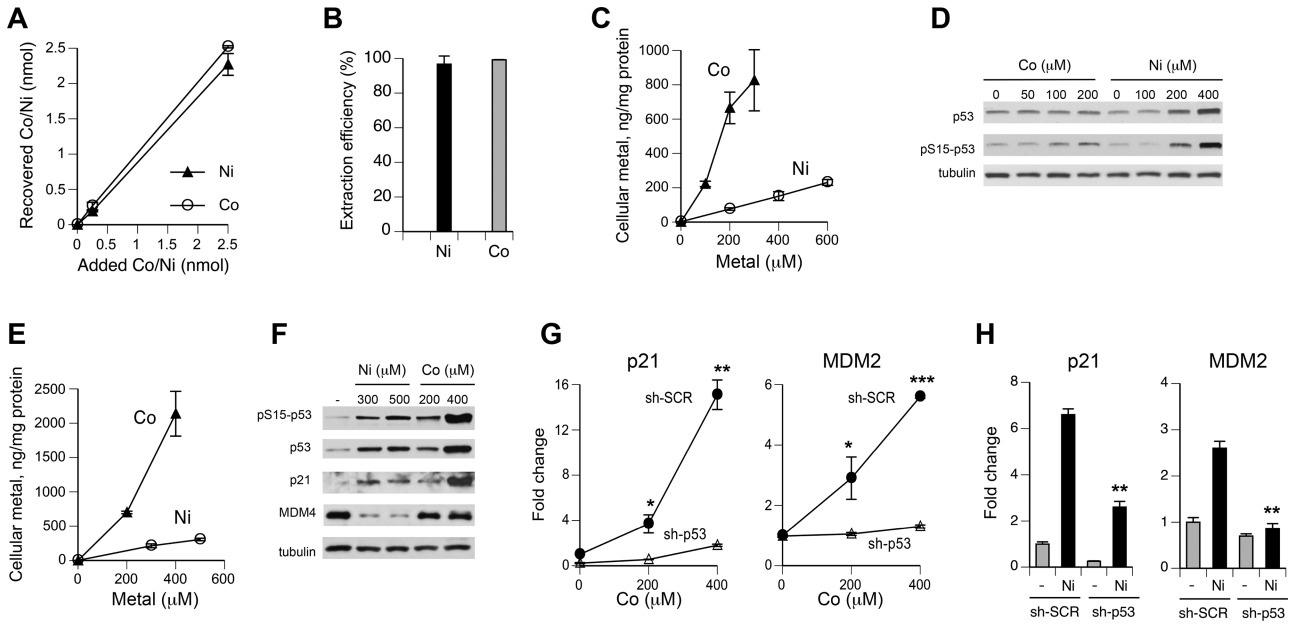

FIG. 1. Metal uptake and p53 activation by Co(II) and Ni(II) in H460 cells. A, Recovery of Co and Ni from H460 cells "spiked" with metals before nitric acid extraction. Data are means ± SD for 3 replicates. B, Percentage of cellular Co and Ni extracted by nitric acid from H460 cells treated with 200μM Co(II) and 400μM Ni(II) for 6 h (means ± SD for 3 independent samples). A total metal content was determined as a sum of measurements in nitric acid–extractable and insoluble fractions. C, Uptake of Co and Ni by H460 cells after 6-h incubation (means ± SD for 3 independent samples). Where not seen, error bars were smaller than data symbols. D, Western blots of protein extracts from H460 cells treated with Co and Ni for 6 h. E, Levels of Co and Ni in H460 cells treated for 24 h (means ± SD for 3 independent samples). Where not seen, error bars were smaller than data symbols. F, Western blots of protein extracts from H460 cells treated with Co and Ni for 24 h. mRNA levels of p21 and MDM2 in H460 cells after 24-h exposure to Co (G) and Ni (H). Data are means ± SD for 2 independent RNA preparations. $*p < 0.05$, $**p < 0.01$, and $***p < 0.001$ relative to the same concentration in sh-SCR samples.

delivering 10 times more intracellular metal had no effect on MDM4 protein (Fig. 1F). Upregulation of p21 and MDM2 mRNA levels by 400μM Ni(II) was more than 2 times lower compared with 400μM Co(II) (Fig. 1H vs Fig. 1G), which is consistent with stronger p53 stabilization and Ser15 phosphorylation in Western blots for this dose of Co(II) (Fig. 1F). However, considering almost 8 times higher cellular doses of Co(II) (Fig. 1E), uptake-normalized induction of MDM2 and p21 by Ni(II) was about 4 times stronger. Similar to Co(II), upregulation of MDM2 and p21 gene expression by Ni(II) was suppressed by p53 depletion (Fig. 1H). Overall, our results showed that in comparison to Ni(II), Co(II) displayed a much higher accumulation in H460 human lung cells, but its activation of the stress-responsive transcription factor p53 was delayed and weaker when normalized for uptake.

Delayed Cytotoxicity by Co(II)

A very strong upregulation of the transcriptional factor p53 by 24-h treatment with 400μM Co(II) prompted us to investigate the presence of apoptotic responses. Surprisingly, we found no increase in activity of the 2 main executioner caspases, caspase-3 and caspase-7, in H460 cells treated with 400μM and higher Co(II) concentrations (Fig. 2A). In contrast, Ni(II)-treated cells displayed a very strong upregulation of caspase activity. The addition of EDTA prior to assay reagents did not significantly change caspase activity readings, arguing against the possibility that negative findings for Co(II) were caused by its interference with the assay. Caspase activity results were corroborated by the absence of a cleaved (active) form of caspase-7 in Co(II)-exposed cells (Fig. 2B). Ni-treated cells contained large amounts of cleaved caspase-7, demonstrating a much greater ability of this metal to engage apoptosis. The absence of caspase activation does not exclude a possibility of other modes of cell death. Any form of cell death would decrease the number of attached cells, which can serve as a test for cell death responses. We found that 24-h treatments with Co(II) caused a dose-dependent suppression of cell proliferation, as evidenced by progressively smaller increases in the number of attached cells (Fig. 2C). However, even the highest dose of 600μM Co(II) did not decrease the number of cells below the pretreatment level. In contrast, losses of cells were detected at 24 h posttreatment, pointing to delayed cell death responses. Assessment of LDH leakage from Co(II)-exposed cells showed no cytotoxicity immediately after 24-h treatments but provided a clear evidence of cell death at 24 h posttreatment (Fig. 2D). A downward trend for LDH readings in samples analyzed at the end of 24-h exposures raised a concern that the presence of Co(II) in media could have interfered with the LDH assay. To test this possibility, we measured activity of the kit-supplied LDH standard in the presence of 400μM Co(II) and found no inhibitory effect (Fig. 2E). Therefore, a modest decrease in LDH activity in samples collected immediately at

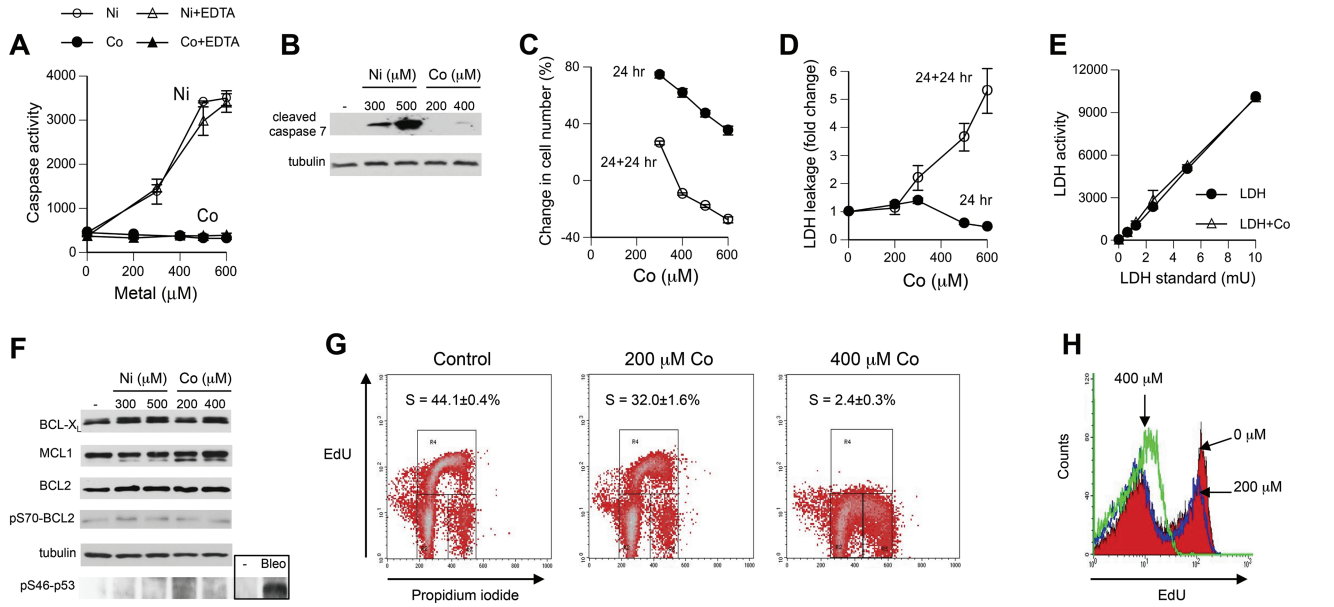

FIG. 2. Cytotoxicity and cell cycle changes in response to Co(II). A, Caspase 3/7 activity in H460 cells treated with Co(II) and Ni(II) for 24 h (means ± SD for 4 independent determinations). In samples labeled Co + EDTA and Ni + EDTA, assay reagents were added after 5-min chelation of metals with 2mM EDTA. B, Formation of active (cleaved) caspase-7 in H460 cells treated with Ni(II) and Co(II) for 24 h. C, Changes in the number of attached cells at the end of 24-h exposures relative to the pre-exposure level ("24 h" line) and after 24-h recovery relative to 0-h recovery ("24 + 24 h" line). The amounts of cells were determined by the CyQUANT reagent. Data are means ± SD for 4 independent determinations. In most cases, error bars were smaller than data symbols. D, Leakage of cellular LDH during 24-h exposure ("24 hr" line) and during 24-h recovery ("24 + 24 hr" line). Data and means ± SD for 4 independent determinations. E, Activity of LDH standard preincubated with or without 400μM Co(II) for 2 h (means ± SD for 4 replicates). F, Westerns blots of protein extracts from H460 cells treated with Ni and Co for 24 h. Bleo: cells were treated with 30 μg/ml bleomycin for 24 h. G, Representative 2-parameter fluorescence-activated cell sorting (FACS) profiles of H460 cells treated with 0–400μM Co(II) for 24 h. EdU incorporation is a measure of DNA replication, whereas propidium iodide is a general DNA stain. EdU (10μM) was added for 30 min after removal of Co(II)-containing media. S-phase values are means ± SD for 3 independent samples. H, FACS profiles of EdU incorporation into H460 cells treated with 0–400μM Co(II) for 24 h.

the end of 24-h exposures most likely reflected lower background readings due to smaller numbers of cells (Fig. 2C). To explore potential reasons for the lack of apoptotic responses at the end of Co(II) exposures, we investigated expression of 3 main antiapoptotic proteins: BCL2, BCL-X_L, and MCL1. Levels of MCL1 are particularly susceptible to regulatory changes, including via its stability controlled by the aminoterminal PEST domain (Domina *et al.*, 2004). PEST domain is defined as a protein region that is rich in proline (P), glutamic acid (E), serine (S), and threonine (T). We found no changes in expression of BCL2, BCL-X_L, and MCL1 in either Ni(II)-treated or Co(II)-treated cells (Fig. 2F). Antiapoptotic phosphorylation of BCL2 at Ser70 was also unaltered by both metals. Although Ni(II)-induced apoptosis in H460 cells involves a mitochondrial pathway (Wong *et al.*, 2013), a clearly different apoptotic proficiency of Ni(II) and Co(II) does not appear to be related to the status of mitochondria-protecting antiapoptotic proteins. Both Ni(II)- and Co(II)-treated cells lacked proapoptotic phosphorylation of p53 at Ser46 (Fig. 2F), which is targeted by a DNA damage–responsive kinase HIPK2 (D'Orazi *et al.*, 2002). The inability of hypoxia-mimicking Co(II) and Ni(II) ions to promote this modification could be related to the absence of DNA damage by these nongenotoxic metals or results from their induction of HIF-1α, which causes destabilization of HIPK2 (Nardinocchi *et al.*, 2011).

To further understand tolerance of Co(II) by H460 cells, we examined inhibition of cell cycle progression, a response that has a lower threshold than cell death and is mechanistically distinct from cell death signaling. We found that 200μM Co(II), a dose delivering 3.3 times more cellular metal than highly apoptotic 500μM Ni(II), produced only modest decreases in the percentage of S-phase cells and the rate of DNA replication (Figs. 2G and 2H). Incubation of H460 cells with 400μM Co(II), which induced a very strong upregulation of p53 and p21 (Fig. 1F), caused a practically complete shutdown of DNA replication. Overall, our results showed that Ni(II) was a much more rapid and potent activator of apoptosis than Co(II). H460 cells loaded with high doses of Co(II) were able to continue replication and display delayed cell death responses.

Cytotoxicity of Co(II) Versus Ni(II)

Different cell viability measurements showed a delayed activation of cell death by Co(II), whereas Ni(II) caused a strong apoptotic response already at the end of 24-h exposure (Fig. 2). Viability of Ni(II)-treated H460 cells continued to decrease at 24 h postexposure and then showed a sharp recovery at 48 h postexposure (Fig. 3A). Co(II) caused a more modest decrease in cell viability at 24 h postexposure and a clear recovery trend after additional 24-h recovery (Fig. 3B). To compare

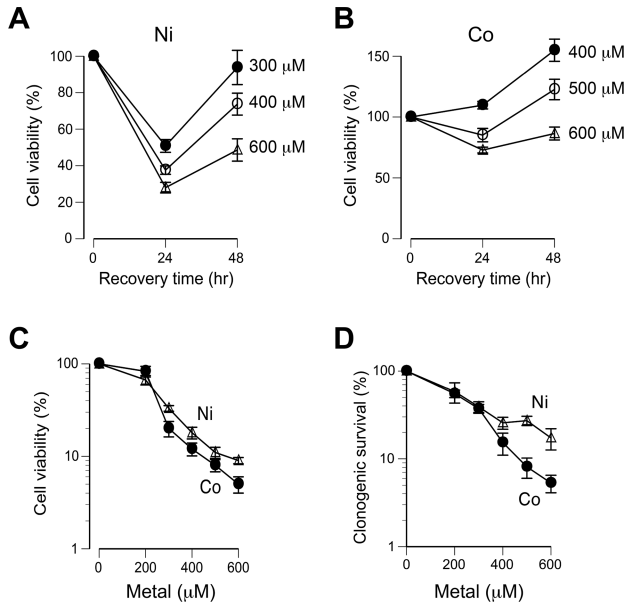

FIG. 3. Comparison of Co(II) and Ni(II) cytotoxicity in H460 cells. In all experiments, cells were treated with metals for 24 h in complete growth media. Viability was assessed by the determination of the metabolic activity of cell populations using the CellTiter-Glo luminescent assay, which measured total cellular ATP levels in a sample. Changes in cell viability at different times after exposure to Ni(II) (A) and Co(II) (B). Data are means ± SD for 6 independent determinations. C, Cell viability at 72 h postexposure (means ± SD for 6 independent determinations). D, Clonogenic survival of H460 cells (means ± SD for 3 independent determinations). Clonogenic viability assesses the ability of cells to retain long-term proliferative activity, as scored by the presence of colonies resulting from proliferation of individual cells. Cells were treated with metals in mass cultures for 24 h, 400 cells from combined populations of attached and floating cells were seeded per 60-mm dish and then grown for 7 days to form visible colonies.

cytotoxicity of Co(II) and Ni(II), we examined cell viability at 72 h postexposure, a time interval incorporating both (1) acute and delayed phases of death and (2) 48-h period of growth recovery for both metals. We found that Co(II) was slightly more cytotoxic than Ni(II) with a 1.1-fold difference in slopes (Fig. 3C). Finally, we measured a long-term viability of Co(II)- and Ni(II)-treated H460 cells by scoring their cloning abilities. To be consistent with uptake measurements, cells were treated with metals in mass cultures for 24 h and then 400 cells from the mixed population of attached and floating cells were seeded per dish for clonogenic survival. From the slopes of dose-response curves, clonogenic toxicity of Co(II) was 1.8 times higher in comparison with Ni(II) (Fig. 3D). Interestingly, a greater toxicity of Co(II) was apparent only at doses with >60% lethality. After normalization for uptake differences (shown in Fig. 1E), Co(II) was on average 7.8 times less toxic than Ni(II) based on cell viability measurements at 72 h postexposure. In clonogenic experiments, uptake-normalized toxicity of Co(II) was lower compared with Ni by 8.6-fold at the low-dose range and 4.8-fold at doses with less than 40% survival. Overall, viability and clonogenic survival data demonstrated a higher tolerance of Co(II) relative to Ni(II) in H460 cells.

Role of p53 in Cytotoxicity of Co(II)

Activation of p53 has been found to play a critical role in Ni(II)-induced apoptosis in H460 cells (Wong *et al.*, 2013), and there was clear evidence of p53 upregulation by Co(II) (Fig. 1F). Therefore, we next investigated whether p53 is important for manifestation of cytotoxic effects by Co(II) using H460 cells with p53 knockdown by shRNA. Consistent with the findings in parental H460 (Figs. 2A and 2B), both cells with control (sh-SCR) and targeting (sh-p53) shRNA contained no detectable cleaved (active) forms of caspase-3 and caspase-7 at the end of 24-h treatments with Co(II) (Fig. 4A). The same result was obtained in repeat Western blots of these samples along with positive controls (not shown). The highest dose of 500μM Co(II) generated a minor cleavage of PARP, which was eliminated by p53 knockdown. At 24 h posttreatment, Co(II)-treated cells expressing control shRNA contained significant amounts of active caspase-3 and caspase-7 and showed a nearly complete PARP cleavage by 500μM Co(II) (Fig. 4B). Cells with p53 knockdown had approximately 2 times lower amounts of active caspases 3/7 and cleaved PARP. The partial dependence of caspase activation on p53 was not a result of its incomplete knockdown because p53 protein and phospho-Ser15 levels were almost undetectable (Figs. 4A and 4B). A complete loss of caspase-3 cleavage by Ni(II) in sh-p53 cells provided a functional validation of their severe p53 deficiency (Fig. 4C). The presence of p53 had no effect on cell growth inhibition by Co(II) during 24-h exposure time (Fig. 4D, top panel), which is consistent with the delayed upregulation of the p53 pathway (Fig. 1). However, knockdown of p53 diminished suppression of cell proliferation and decreased the loss of cells (cell death) during 24-h recovery in Co(II)-free media (Fig. 4D, bottom panel). In agreement with Western blotting results for cleaved caspases, p53 depletion diminished caspase 3/7 activity in Co(II)-treated cells by approximately 2-fold (Fig. 4E). Finally, we determined that p53 deficiency increased cell death resistance to Co(II), as evidenced by lower levels of LDH leakage and a higher clonogenic survival (Figs. 4F and 4G). Overall, our results showed that upregulation of p53 was responsible for 50%–60% of caspase 3/7 activation and cell death by Co(II). Caspase-3 activation by Ni(II) was completely dependent on p53.

To further understand mechanisms of Co(II)-induced apoptosis, we measured mRNA levels for 12 major pro- and antiapoptotic proteins. Stress-induced apoptosis can be executed via mitochondrial (intrinsic) or death receptor–mediated (extrinsic) mechanism. The key event in the intrinsic form of apoptosis is release of proapoptotic factors from mitochondria by oligomers of BAX and BAK that form pores in the outer mitochondrial membrane. Oligomerization of BAX/BAK is promoted by BH3-only domain proteins (PUMA, NOXA, BID, and BIM) and suppressed by BH4-containing proteins such as BCL2 and MCL1 (Green and Kroemer, 2009). Mitochondria-dependent apoptosis engages the initiator caspase-9. We found that irrespective of their p53 status, Co(II)-treated cells showed no

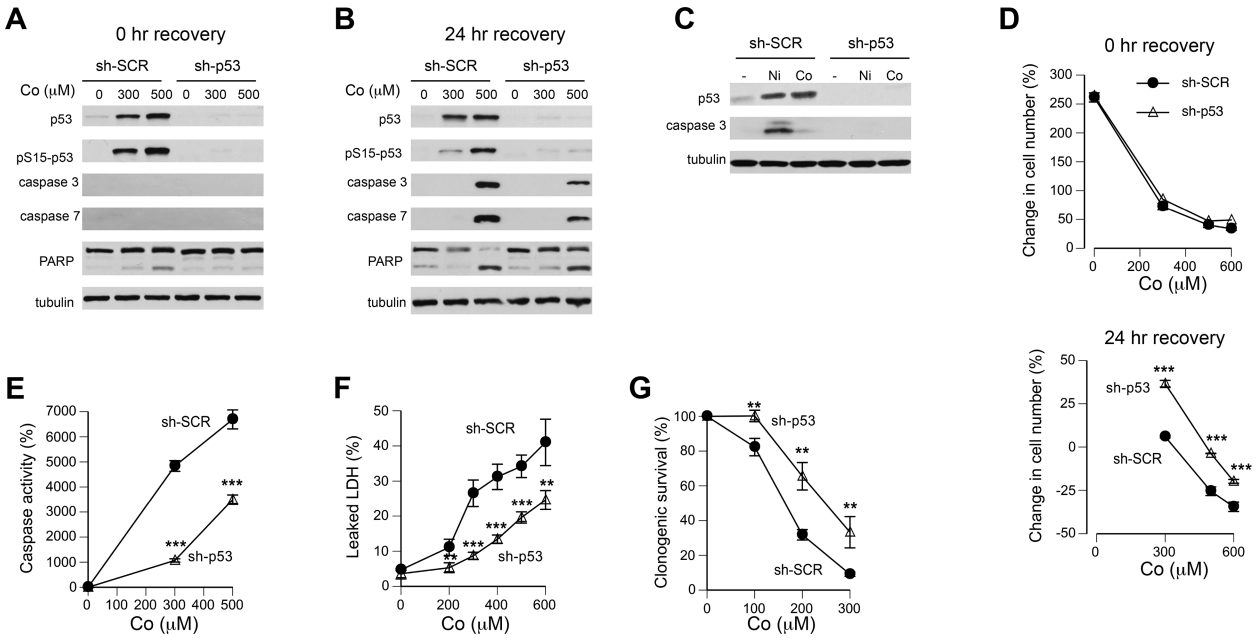

FIG. 4. Role of p53 in cytotoxicity of Co(II) in H460 cells. A, Western blots for samples collected at the end of 24-h treatments with Co(II) (sh-SCR—cells expressing nonspecific shRNA and sh-p53—cells with p53-targeting shRNA). B, Western blots for samples collected at 24 h posttreatment. C, Western blots for p53 and cleaved (active) caspase-3 in cells treated with 250 μM Ni(II) or Co(II) for 48 h. D, Effect of p53 depletion on growth inhibition by Co(II) at the end of 24-h treatments (top panel) and following 24-h recovery in metal-free media (bottom panel). Means ± SD for 4 independent determinations. ***$p < 0.001$ relative to the same concentration in sh-SCR samples. Error bars were smaller than data symbols in most cases. E, Caspase 3/7 activity in H460 cells following 24-h recovery in Co-free media. Means ± SD for 4 independent determinations. ***$p < 0.001$ relative to the same concentration in sh-SCR samples. F, LDH leakage from H460 cells during 24 h posttreatment incubation. Means ± SD for 4 independent determinations. **$p < 0.01$ and ***$p < 0.001$ relative to the same concentration in sh-SCR samples. G, Clonogenic survival of H460 cells treated with Co(II) for 24 h. Means ± SD for 3 independent determinations. **$p < 0.01$ relative to the same concentration in sh-SCR samples.

significant changes in gene expression for caspase-9, as well as its adaptor protein APAF1 and inhibitor BIRC5 (survivin, IAP4) (Fig. 5A). Messenger RNA levels for antiapoptotic MCL1 and BCL2 were also similar in both control and p53-depleted cells (Fig. 5B). Examination of gene expression for BH3-only activators of BAX/BAK oligomerization found that Co(II) caused a strong upregulation of NOXA (PMAIP1) and PUMA (BBC3) mRNA and this response was suppressed in sh-p53 cells by approximately 60% (Fig. 5C). Co(II)-treated cells also showed a modest, p53-independent increase in BIM expression but a slight decrease in BID. There was no effect of Co(II) on mRNA amounts of apoptotic BAX although its expression was moderately lower in p53 knockdown cells. Overall, our qRT-PCR analyses found that upregulation of NOXA and PUMA was the main proapoptotic gene expression response in Co(II)-treated cells. Induction of these genes was partially dependent on p53.

Mechanisms of Cell Death by Co(II)

Leakage of cellular LDH, which we observed in Co(II)-treated cells (Fig. 2D), can reflect the presence of late apoptotic cells or induction of necrosis. Co(II) is a prooxidant metal (Kasprzak *et al.*, 2003), and oxidative stress is known to promote a necrotic death via opening of the mitochondrial permeability transition pore and subsequent collapse of the H^+ gradient and loss of ATP production. Importantly, p53 protein induces this form of necrosis by binding to cyclophilin D in the inner mitochondrial membrane (Vaseva *et al.*, 2012). Thus, it was plausible that the observed above inhibition of LDH leakage in sh-p53 H460 cells (Fig. 4F) was caused by a suppression of p53-dependent necrosis. Using different pharmacological agents, we next explored a role of necrotic and caspase-dependent and -independent processes in Co(II) cytotoxicity. The extent of cell death was monitored by LDH leakage at 24 h postexposure, which corresponds to the peak of Co(II)-induced cytotoxicity (Figs. 3 and 4). In the initial screening, inhibitors were added only for 24-h recovery time to avoid potential effects on Co(II) uptake. We found that addition of cyclosporine A, which blocks physical interactions between p53 and cyclophilin D and oxidant-induced necrosis (Vaseva *et al.*, 2012), had no effect on LDH release from Co(II)-treated H460 cells (Fig. 6A). LDH leakage was also unchanged in the presence of necrostatin-1, which inhibits a death receptor–associated form of necrosis involving RIP1 (RIPK1) kinase (Degterev *et al.*, 2008). Consistent with the observed earlier activation of executioner caspases, the pancaspase inhibitor QVD-Oph suppressed LDH leakage by more than 60%. Inhibition of other cysteine proteases, such as cytosolic calpains by ALLN and lysosomal cathepsins by E64d, had no effect on the amount of extracellular LDH. Western blotting results demonstrated a complete blockage of

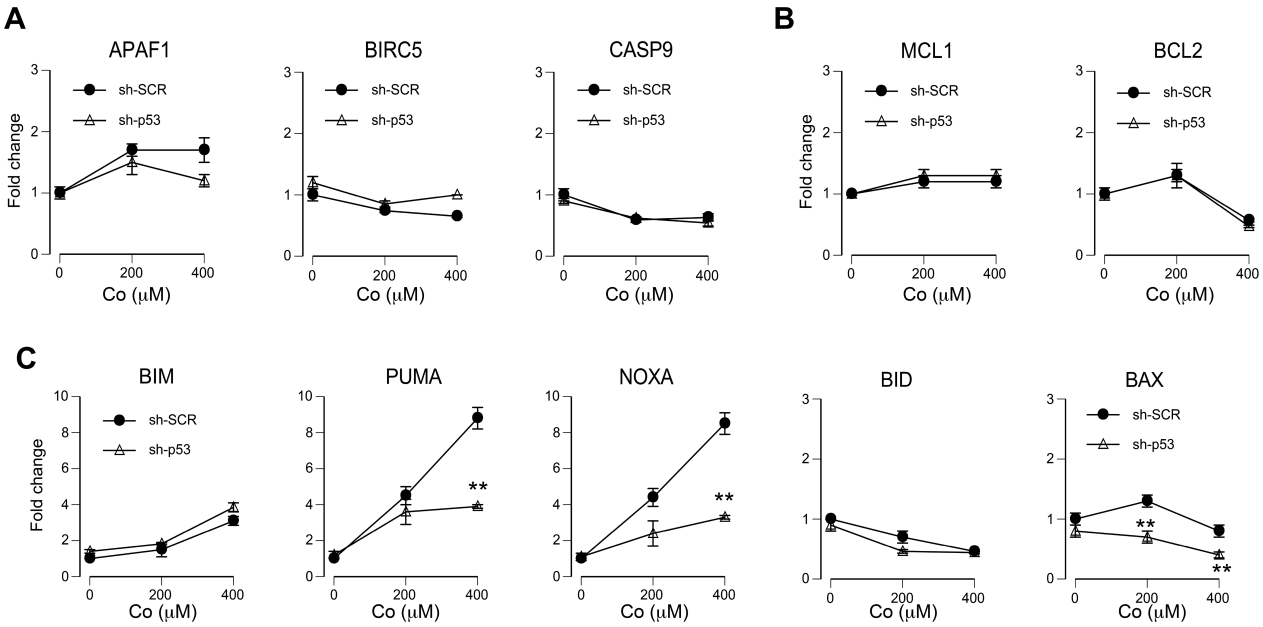

FIG. 5. qRT-PCR for apoptosis-related genes in Co(II)-treated H460 cells. Total RNA was isolated from cells expressing nonspecific (sh-SCR) and p53-targeting shRNA (sh-p53) following Co(II) treatments for 24 h. Data are means ± SD for 2 independent RNA preparations (**$p < 0.01$ relative to the same concentration in sh-SCR samples). A, mRNA levels for proteins associated with caspase-9 activation. B, Gene expression for antiapoptotic MCL1 and BCL2. C, Gene expression for proapoptotic BAX- and BH3-domain-containing activators.

PARP cleavage and the production of active caspases 3/7 by QVD-Oph (Fig. 6B). The presence of ALLN and E64d did not change the levels of these apoptotic markers, excluding the role of cathepsins and calpains in the initiation of caspase activation. Next, we examined whether the incompleteness of LDH release and the inhibitory effects of QVD-Oph were caused by its presence only during 24-h recovery, which could have allowed some early apoptotic events. We found that the degree of LDH inhibition was not affected by the addition of QVD-Oph during and after Co(II) exposure versus only during postexposure time (Fig. 6C, left panel). Control experiments showed that cytotoxicity-inhibitory effects of QVD-Oph were not associated with suppressive effects on p53 accumulation (Fig. 6C, right panel). Finally, we examined a relative role of p53- and caspase-dependent processes in cell death by Co(II) (Fig. 6D). From the slopes of dose-response curves, we calculated that p53 depletion inhibited LDH leakage by about 55% and QVD-Oph by approximately 75% in both control and sh-p53 cells. Overall, our results showed that cell death by Co(II) involved multiple mechanisms and was partially dependent on p53.

Co(II) and Ni(II) Treatments of Normal Human Lung Cells

To confirm our findings in H460 cells, we examined uptake of Ni(II) and Co(II) in IMR90 normal human lung fibroblasts and primary HBE cells. We found that both types of normal lung cells had several times higher accumulation of Co(II) than Ni(II) (Figs. 7A and 7B). Ni(II)-treated HBE cells showed a dose-dependent increase in caspase 3/7 activity at the end of 24-h exposures (Fig. 7C). In contrast, despite its much higher cellular doses, Co(II) produced no caspase activation. In agreement with findings in H460, Co(II)-treated HBE cells displayed a moderate activation of caspases at 24 h postexposure (Fig. 7D). Thus, studies with 2 types of normal human lung cells confirmed a much higher uptake of Co(II) but a delayed and weaker caspase activation compared with Ni(II).

DISCUSSION

Co(II)-Induced Cell Death

Our studies here showed that despite their chemical similarity, Co(II) had a much higher cellular accumulation than Ni(II), but it was a slower and weaker activator of p53 and death in H460 cells. In contrast to Ni(II), even several times higher cellular doses of Co(II) produced no changes in the levels of the p53 inhibitor MDM4, indicating activation of a more limited stress signaling network. Delayed death in Co(II)-treated cells was triggered via p53-dependent and -independent mechanisms (Fig. 8A). Approximately 55% of Co(II)-induced cell death was attributable to the p53-dependent, caspase-mediated apoptosis. This conclusion was drawn from the inhibition of caspase activity, decreases in active caspase-3 and caspase-7, and suppression of LDH release by p53 knockdown. Consistent with the above estimate, Co(II)-induced expression of 2 most highly upregulated proapoptotic genes NOXA and PUMA was reduced by 50%–60% in

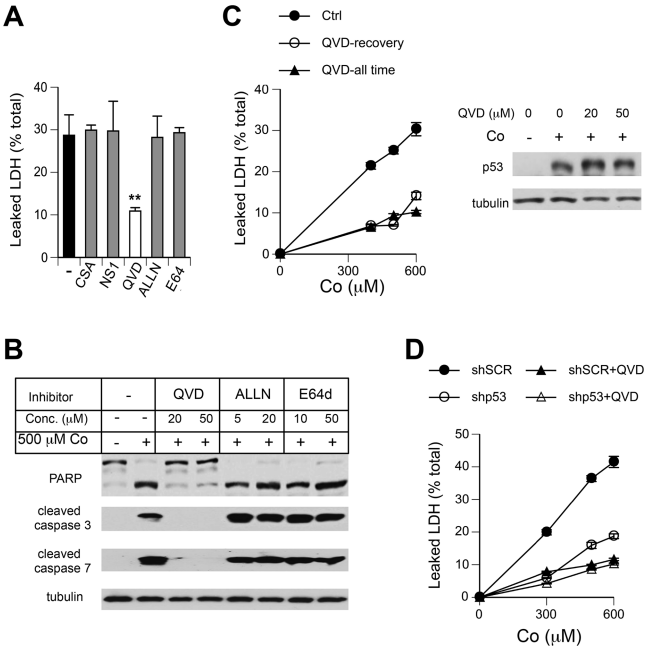

FIG. 6. Mechanisms of death in Co(II)-treated H460 cells. Data are means ± SD for at least 3 independent determinations. Where not seen, error bars were smaller than data symbols. A, Leaked LDH from cells treated with 500μM Co(II) for 24h in complete media and then incubated for 24h in metal-free media without serum in the presence of inhibitors: CSA—cyclosporin A (4μM), NS1—necrostatin-1 (10μM), QVD (QVD-Oph, 20μM), ALLN (5μM), and E64d (10μM). $^{**}p < 0.01$ relative to Co(II)-treated cells without inhibitors. B, Formation of active caspases 3/7 and PARP cleavage in cells treated with Co(II) and inhibitors as in panel A. C, Inhibition of LDH leakage by 50μM QVD-Oph present during and after Co(II) treatment (QVD-all time) and added only for 24-h recovery (QVD-recovery). Right panel: p53 protein levels in H460 cells treated with QVD-Oph during 24 h Co(II) exposure and 24 h postexposure. D, LDH leakage from cells with control (sh-SCR) and p53-targeting (sh-p53) shRNA in the presence or absence of 50μM QVD-Oph (QVD, present during and after exposure). LDH leakage was measured after 24-h recovery in Co(II)-free media.

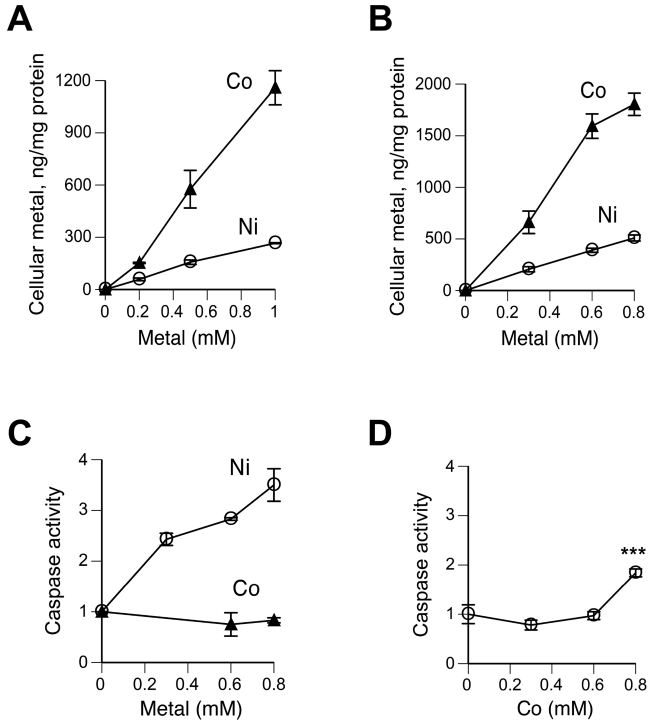

FIG. 7. Treatments of normal human lung cells with Co(II) and Ni(II). Cells were treated with metals for 24h. Data are means ± SD for at least 3 independent determinations. A, Accumulation of metals by IMR90 normal human fibroblasts and B, primary HBE cells. C, Caspase activity in HBE cells after 24-h exposure to metals. D, Caspase activity in HBE cells at 24h postexposure to Co(II) ($^{***}p < 0.001$ relative to untreated cells).

p53-depleted cells. Unlike Ni(II) (Wong *et al.*, 2013), loss of p53 did not cause derepression of antiapoptotic MCL1 by Co(II), which together with only a partial effect on PUMA induction and caspase-3 activation was probably responsible for the overall less potent prosurvival effect of p53 deficiency for Co(II). A caspase-mediated but p53-independent apoptosis accounted for about 20% of Co(II)-induced cell death, and the remaining 25% death was both p53 and caspase independent. In contrast to engagement of multiple cell death mechanisms by Co(II), our recent studies showed that Ni(II)-induced death in H460 cells was entirely caspase dependent, and p53 depletion completely abrogated caspase-3 activation (Wong *et al.*, 2013). Although Co(II) is a redox-active metal and oxidative stress is known to activate necrosis by p53 binding to mitochondrial cyclophilin D (Vaseva *et al.*, 2012), we did not detect any survival benefit by inhibiting this and alternative RIP1-dependent (Vandenabeele *et al.*, 2010) necrotic pathways. Our findings on a similar residual cytotoxicity in control and p53-depleted cells in the presence of the pancaspase inhibitor QVD-Oph further argue against any pronecrotic effect of p53 in Co(II)-treated cells. Because p53 deficiency did not completely suppress NOXA and PUMA induction, it is possible that the continuing mitochondrial release of cytotoxic proteins such as endonuclease G and AIF promoting apoptosis directly (Green and Kroemer, 2009) was responsible for the caspase-resistant cell death by Co(II). Alternatively, caspase-inhibited severely injured cells could become nonviable due to a loss of essential respiration factors caused by a persistent permeabilization of the outer mitochondrial membrane (Lartigue *et al.*, 2009). Human lung cells accumulated 4–9 times more Co(II) than Ni(II), as determined by direct measurements of cellular metals in our studies. The indirectly measured rates of Co^{2+} influx by the human divalent metal transporter DMT1 expressed in *Xenopus* oocytes were 4.9–7.0 times higher than for Ni^{2+} (Illing *et al.*, 2012). Similar estimates for transport preference of Co(II) over Ni(II) points to the importance of DMT1 in metal uptake by lung cells. Metal selectivity for Co(II) and Ni(II) entry via other transporters such as Ca^{2+} channels is currently unknown (Goodman *et al.*, 2011; Simonsen *et al.*, 2012).

Our findings on a high tolerance of Co(II) by human lung cells are consistent with a lack of respiratory toxicity in individuals displaying injury to other tissues caused by elevated levels of cobalt in systemic circulation (Gilbert *et al.*, 2013;

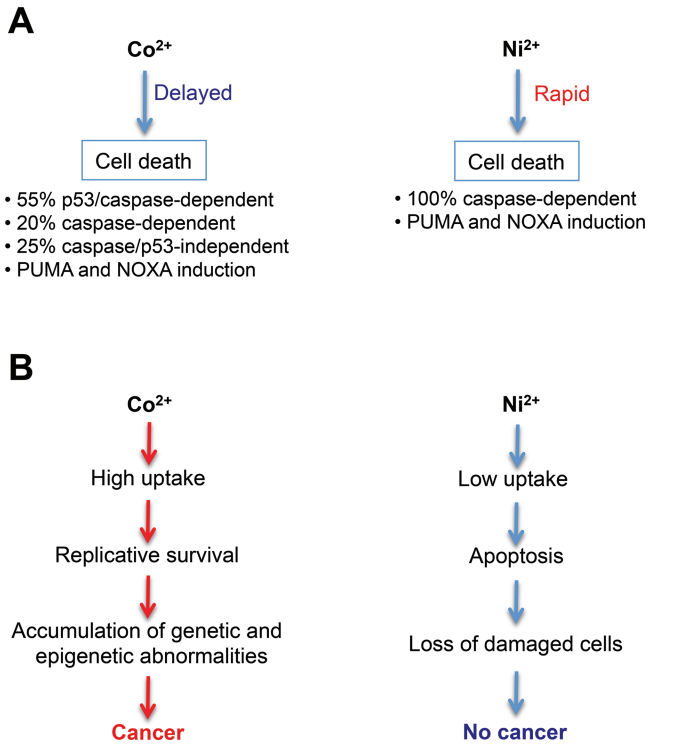

FIG. 8. A, A summary of cell death mechanisms activated by Co(II) and Ni(II) in H460 human lung epithelial cells. Caspase dependence of cell death by Ni(II) was established in our recent publication (Wong *et al.*, 2013). B, A model for the role of cytotoxicity in carcinogenicity of Co(II) and Ni(II) ions.

Simonsen *et al.*, 2012). Resistance of lung cells to Co(II) does not appear to stem from the ability of this metal to suppress cell death as DNA replication was also relatively insensitive to inhibition by Co(II). Co(II) has also shown no inhibitory effect on the induction of apoptosis by cisplatin in kidney cells (Wang *et al.*, 2006). *In vitro* binding of p53 to its consensus sequence was less sensitive to the presence of Co(II) than Ni(II) ions (Palecek *et al.*, 1999), suggesting that a higher cellular tolerance of Co(II) was unlikely a result of a direct inhibition of this proapoptotic factor. Unlike Ni(II), cytotoxic measurements for Co(II) showed sublinear or threshold-like responses in H460 cells at low doses (eg, caspase 3/7 and PARP cleavage in Fig. 4B and LDH leakage in Fig. 4F), suggesting that under these conditions, the majority of cellular Co(II) could be bound by abundant ligands on low-toxicity targets (ie, structural proteins and glutathione). Increasing saturation of these sites at high doses would cause a general deterioration of cellular functions and permit Co(II) binding to low-abundance critical enzymes, producing disproportionately steeper increases in toxicity and the sublinear shape of dose-dependent responses. Although both metals share many similarities in ligand binding (Nieboer and Richardson, 1980), sterically restrictive tetrahedral and especially octahedral geometry of Co(II) probably favors binding at the exterior of proteins, which is expected to be weakly structure disruptive. A more toxic Ni(II) forms a larger assortment of ligand arrangements, and its common square planar structure permits a peptide-specific binding and protein cleavage, which is not observed for Co(II) (Bal *et al.*, 2000).

Implications for Ni(II) and Co(II) Carcinogenicity

The intracellular release of Ni(II) ions is generally believed to be responsible for cancer causation by insoluble Ni compounds, although epidemiological data for carcinogenicity of soluble Ni(II) are largely negative (Goodman *et al.*, 2011; Muñoz and Costa, 2012; Salnikow and Zhitkovich, 2008). Soluble Ni(II) (nickel sulfate) was also noncarcinogenic by inhalation in the 2-year rodent carcinogenicity assay (Dunnick *et al.*, 1995). In contrast, inhalation exposures to the same doses of soluble Co(II) (cobalt sulfate) caused lung tumors in both mice and rats (Bucher *et al.*, 1999). Co(II) is clastogenic *in vivo* and in cultured cells, and this genotoxic activity has been attributed to oxidative damage (De Boeck *et al.*, 2003). Co(II) is generally more redox active than Ni(II), and cells treated with Co(II) showed higher levels of oxidative stress (Kasprzak *et al.*, 2003; Van den Broeke *et al.*, 1998). A high tolerance of intracellular Co(II) by lung cells, including resistance of DNA synthesis, can allow their propagation despite the presence of oxidative damage, which should promote accumulation of critical amounts of genetic rearrangements and stimulate transformation of surviving cells (Fig. 8B). A lower threshold and more rapid activation of apoptosis by soluble Ni(II) helps eliminate damaged cells prior to their acquiring of procarcinogenic genetic or epigenetic changes. The carcinogenic ability of insoluble Ni compounds is frequently attributed to the intracellular delivery of massive amounts of Ni(II) ions upon dissolution of micron-sized particles. Our data on high cytotoxicity of Ni(II) ions would argue that in addition to their gradual release from slowly dissolving particles, a major fraction of Ni(II) leaking from endosomes into cytosol and nuclear compartments could be bound by ligands, blunting cytotoxicity of Ni(II) ions but retaining or enhancing their carcinogenic properties. Ni(II) binding to histidine and other small molecules is known to enhance its oxidative chemistry (Kasprzak *et al.*, 2003), but this complexation should diminish reactivity of Ni with proteins, limiting the overall cellular injury and permitting survival.

FUNDING

National Institute of Environmental Health Sciences (ES008786, ES013660).

ACKNOWLEDGMENTS

A. Z. served as a consultant to Lynntech Inc for U.S. Air Force–sponsored research project on chromium in 2012–2013.

REFERENCES

Bal, W., Liang, R., Lukszo, J., Lee, S. H., Dizdaroglu, M., and Kasprzak, K. S. (2000). Ni(II) specifically cleaves the C-terminal tail of the major variant of histone H2A and forms an oxidative damage-mediating complex with the cleaved-off octapeptide. *Chem. Res. Toxicol*. **13,** 616–624.

Bal, W., Schwerdtle, T., and Hartwig, A. (2003). Mechanism of nickel assault on the zinc finger of DNA repair protein XPA. *Chem. Res. Toxicol*. **16,** 242–248.

Bucher, J. R., Elwell, M. R., Thompson, M. B., Chou, B. J., Renne, R., and Ragan, H. A. (1990). Inhalation toxicity studies of cobalt sulfate in F344/N rats and B6C3F1 mice. *Fundam. Appl. Toxicol*. **15,** 357–372.

Bucher, J. R., Hailey, J. R., Roycroft, J. R., Haseman, J. K., Sills, R. C., Grumbein, S. L., Mellick, P. W., and Chou, B. J. (1999). Inhalation toxicity and carcinogenicity studies of cobalt sulfate. *Toxicol. Sci*. **49,** 56–67.

De Boeck, M., Kirsch-Volders, M., and Lison, D. (2003). Cobalt and antimony: Genotoxicity and carcinogenicity. *Mutat. Res*. **533,** 135–152.

Degterev, A., Hitomi, J., Germscheid, M., Ch'en, I. L., Korkina, O., Teng, X., Abbott, D., Cuny, G. D., Yuan, C., Wagner, G., *et al.* (2008). Identification of RIP1 kinase as a specific cellular target of necrostatins. *Nat. Chem. Biol*. **4,** 313–321.

Delaunay, C., Petit, I., Learmonth, I. D., Oger, P., and Vendittoli, P. A. (2010). Metal-on-metal bearings total hip arthroplasty: The cobalt and chromium ions release concern. *Orthop. Traumatol. Surg. Res*. **96,** 894–904.

Domina, A. M., Vrana, J. A., Gregory, M. A., Hann, S. R., and Craig, R. W. (2004). MCL1 is phosphorylated in the PEST region and stabilized upon ERK activation in viable cells, and at additional sites with cytotoxic okadaic acid or taxol. *Oncogene* **23,** 5301–5315.

D'Orazi, G., Cecchinelli, B., Bruno, T., Manni, I., Higashimoto, Y., Saito, S., Gostissa, M., Coen, S., Marchetti, A., Del Sal, G., *et al.* (2002). Homeodomain-interacting protein kinase-2 phosphorylates p53 at Ser 46 and mediates apoptosis. *Nat. Cell Biol*. **4,** 11–19.

Dunnick, J. K., Elwell, M. R., Radovsky, A. E., Benson, J. M., Hahn, F. F., Nikula, K. J., Barr, E. B., and Hobbs, C. H. (1995). Comparative carcinogenic effects of nickel subsulfide, nickel oxide, or nickel sulfate hexahydrate chronic exposures in the lung. *Cancer Res*. **55,** 5251–5256.

Gilbert, C. J., Cheung, A., Butany, J., Zywiel, M. G., Syed, K., McDonald, M., Wong, F., and Overgaard, C. (2013). Hip pain and heart failure: The missing link. *Can. J. Cardiol*. **29,** 639.e1–639.e2.

Goodman, J. E., Prueitt, R. L., Thakali, S., and Oller, A. R. (2011). The nickel ion bioavailability model of the carcinogenic potential of nickel-containing substances in the lung. *Crit. Rev. Toxicol*. **41,** 142–174.

Green, D. R., and Kroemer, G. (2009). Cytoplasmic functions of the tumour suppressor p53. *Nature* **458,** 1127–1130.

Huang, X., Kitahara, J., Zhitkovich, A., Dowjat, K., and Costa, M. (1995). Heterochromatic proteins specifically enhance nickel-induced 8-oxo-dG formation. *Carcinogenesis* **16,** 1753–1759.

Illing, A. C., Shawki, A., Cunningham, C. L., and Mackenzie, B. (2012). Substrate profile and metal-ion selectivity of human divalent metal-ion transporter-1. *J. Biol. Chem*. **287,** 30485–30496.

Kasprzak, K. S., Sunderman, F. W., Jr, and Salnikow, K. (2003). Nickel carcinogenesis. *Mutat. Res*. **533,** 67–97.

Kopera, E., Schwerdtle, T., Hartwig, A., and Bal, W. (2004). Co(II) and Cd(II) substitute for Zn(II) in the zinc finger derived from the DNA repair protein XPA, demonstrating a variety of potential mechanisms of toxicity. *Chem. Res. Toxicol*. **17,** 1452–1458.

Kruse, J. P., and Gu, W. (2009). Modes of p53 regulation. *Cell* **137,** 609–622.

Lartigue, L., Kushnareva, Y., Seong, Y., Lin, H., Faustin, B., and Newmeyer, D. D. (2009). Caspase-independent mitochondrial cell death results from loss of respiration, not cytotoxic protein release. *Mol. Biol. Cell* **20,** 4871–4884.

Messer, J., Reynolds, M., Stoddard, L., and Zhitkovich, A. (2006). Causes of DNA single-strand breaks during reduction of chromate by glutathione in vitro and in cells. *Free Radic. Biol. Med*. **40,** 1981–1992.

Muñoz, A., and Costa, M. (2012). Elucidating the mechanisms of nickel compound uptake: A review of particulate and nano-nickel endocytosis and toxicity. *Toxicol. Appl. Pharmacol*. **260,** 1–16.

Nardinocchi, L., Puca, R., and D'Orazi, G. (2011). HIF-1α antagonizes p53-mediated apoptosis by triggering HIPK2 degradation. *Aging (Albany NY)* **3,** 33–43.

Nieboer, E., and Richardson, D. H. S. (1980). The replacement of the nondescript term "heavy metals" by a biologically and chemically significant classification of metal ions. *Environ. Pollut. Ser. B* **1,** 3–26.

Nordberg, G. (1994). Assessment of risks in occupational cobalt exposures. *Sci. Total Environ*. **150,** 201–207.

Palecek, E., Brázdová, M., Cernocká, H., Vlk, D., Brázda, V., and Vojtesek, B. (1999). Effect of transition metals on binding of p53 protein to supercoiled DNA and to consensus sequence in DNA fragments. *Oncogene* **18,** 3617–3625.

Reynolds, M., Peterson, E., Quievryn, G., and Zhitkovich, A. (2004). Human nucleotide excision repair efficiently removes chromium-DNA phosphate adducts and protects cells against chromate toxicity. *J. Biol. Chem*. **279,** 30419–30424.

Reynolds, M., and Zhitkovich, A. (2007). Cellular vitamin C increases chromate toxicity via a death program requiring mismatch repair but not p53. *Carcinogenesis* **28,** 1613–1620.

Salnikow, K., Blagosklonny, M. V., Ryan, H., Johnson, R., and Costa, M. (2000). Carcinogenic nickel induces genes involved with hypoxic stress. *Cancer Res*. **60,** 38–41.

Salnikow, K., Donald, S. P., Bruick, R. K., Zhitkovich, A., Phang, J. M., and Kasprzak, K. S. (2004). Depletion of intracellular ascorbate by the carcinogenic metals nickel and cobalt results in the induction of hypoxic stress. *J. Biol. Chem*. **279,** 40337–40344.

Salnikow, K., and Zhitkovich, A. (2008). Genetic and epigenetic mechanisms in metal carcinogenesis and cocarcinogenesis: Nickel, arsenic, and chromium. *Chem. Res. Toxicol*. **21,** 28–44.

Simonsen, L. O., Harbak, H., and Bennekou, P. (2012). Cobalt metabolism and toxicology—A brief update. *Sci. Total Environ*. **432,** 210–215.

Toledo, F., and Wahl, G. M. (2006). Regulating the p53 pathway: In vitro hypotheses, in vivo veritas. *Nat. Rev. Cancer* **6,** 909–923.

Van den Broeke, L. T., Gräslund, A., Nilsson, J. L., Wahlberg, J. E., Scheynius, A., and Karlberg, A. T. (1998). Free radicals as potential mediators of metal-allergy: Ni2+- and Co2+-mediated free radical generation. *Eur. J. Pharm. Sci*. **6,** 279–286.

Vandenabeele, P., Galluzzi, L., Vanden Berghe, T., and Kroemer, G. (2010). Molecular mechanisms of necroptosis: An ordered cellular explosion. *Nat. Rev. Mol. Cell Biol*. **11,** 700–714.

Vaseva, A. V., Marchenko, N. D., Ji, K., Tsirka, S. E., Holzmann, S., and Moll, U. M. (2012). p53 opens the mitochondrial permeability transition pore to trigger necrosis. *Cell* **149,** 1536–1548.

Wang, G. L., and Semenza, G. L. (1995). Purification and characterization of hypoxia-inducible factor 1. *J. Biol. Chem*. **270,** 1230–1237.

Wang, J., Biju, M. P., Wang, M. H., Haase, V. H., and Dong, Z. (2006). Cytoprotective effects of hypoxia against cisplatin-induced tubular cell apoptosis: Involvement of mitochondrial inhibition and p53 suppression. *J. Am. Soc. Nephrol*. **17,** 1875–1885.

Wong, V. C., Cash, H. L., Morse, J. L., Lu, S., and Zhitkovich, A. (2012). S-phase sensing of DNA-protein crosslinks triggers TopBP1-independent ATR activation and p53-mediated cell death by formaldehyde. *Cell Cycle* **11,** 2526–2537.

Wong, V. C., Morse, J. L., and Zhitkovich, A. (2013). p53 activation by Ni(II) is a HIF-1α independent response causing caspases 9/3-mediated apoptosis in human lung cells. *Toxicol. Appl. Pharmacol*. **269,** 233–239.

Zhang, D., Zaugg, K., Mak, T. W., and Elledge, S. J. (2006). A role for the deubiquitinating enzyme USP28 in control of the DNA-damage response. *Cell* **126,** 529–542.